PCT

WORLD INTELLECTUAL PROPERTY ORGANIZATION
International Bureau

INTERNATIONAL APPLICATION PUBLISHED UNDER THE PATENT COOPERATION TREATY (PCT)

(51) International Patent Classification 5 :	A1	(11) International Publication Number: WO 94/09383
G01T 1/166		(43) International Publication Date: 28 April 1994 (28.04.94)

(21) International Application Number: PCT/US93/09429

(22) International Filing Date: 30 September 1993 (30.09.93)

(30) Priority data:
07/958,980 9 October 1992 (09.10.92) US

(71) Applicant: THE REGENTS OF THE UNIVERSITY OF CALIFORNIA [US/US]; 300 Lakeside Drive, 22nd Floor, Oakland, CA 94612-3550 (US).

(72) Inventors: HASEGAWA, Bruce, H. ; 2303 Julie Lane, South San Francisco, CA 94080 (US). GOULD, Robert, G. ; 30 Rivoli Street, San Francisco, CA 94117 (US). LANG, Thomas, F. ; 100 Font Boulevard, Apt. 5B, San Francisco, CA 94134 (US). BROWN, J., Keenan ; 1006 Pine Avenue, San Jose, CA 95125 (US). HEANUE, Joseph, A. ; 1717 Hopkins Street, Berkeley, CA 94707 (US). CANN, Christopher, E. ; 53 Carmel Street, San Francisco, CA 94117 (US).

(74) Agent: ROBBINS, Billy, A.; Robbins, Berliner & Carson, 201 North Figueroa Street, 5th Floor, Los Angeles, CA 90012-2628 (US).

(81) Designated States: AT, AU, BB, BG, BR, BY, CA, CH, CZ, DE, DK, ES, FI, GB, HU, JP, KP, KR, KZ, LK, LU, MG, MN, MW, NL, NO, NZ, PL, PT, RO, RU, SD, SE, SK, UA, VN, European patent (AT, BE, CH, DE, DK, ES, FR, GB, GR, IE, IT, LU, MC, NL, PT, SE), OAPI patent (BF, BJ, CF, CG, CI, CM, GA, GN, ML, MR, NE, SN, TD, TG).

Published
With international search report.

(54) Title: EMISSION-TRANSMISSION IMAGING SYSTEM USING SINGLE ENERGY AND DUAL ENERGY TRANSMISSION AND RADIONUCLIDE EMISSION DATA

(57) Abstract

Radionuclide emission imaging is improved by correcting emission-transmission data for attenuation along calculated path lengths and through calculated basis material. X-ray transmission data are used to develop an attenuation map through an object which is then used in reconstructing an image based on emission data. Radiation detection circuitry is provided which has different operating modes in detecting the X-ray and emission photons passing through the object. An iterative process is used to reconstruct the radionuclide distribution using the radionuclide projection data and the attenuation map based on physical characteristics of the object being imaged. Subsets of the complete radionuclide projection data are used to reconstruct image subsets of the radionuclide distribution. The image subsets can be generated concurrently with the acquisition of the radionuclide projection data or following acquisition of all data.

FOR THE PURPOSES OF INFORMATION ONLY

Codes used to identify States party to the PCT on the front pages of pamphlets publishing international applications under the PCT.

AT	Austria
AU	Australia
BB	Barbados
BE	Belgium
BF	Burkina Faso
BG	Bulgaria
BJ	Benin
BR	Brazil
BY	Belarus
CA	Canada
CF	Central African Republic
CG	Congo
CH	Switzerland
CI	Côte d'Ivoire
CM	Cameroon
CN	China
CS	Czechoslovakia
CZ	Czech Republic
DE	Germany
DK	Denmark
ES	Spain
FI	Finland
FR	France
GA	Gabon
GB	United Kingdom
GN	Guinea
GR	Greece
HU	Hungary
IE	Ireland
IT	Italy
JP	Japan
KP	Democratic People's Republic of Korea
KR	Republic of Korea
KZ	Kazakhstan
LI	Liechtenstein
LK	Sri Lanka
LU	Luxembourg
LV	Latvia
MC	Monaco
MG	Madagascar
ML	Mali
MN	Mongolia
MR	Mauritania
MW	Malawi
NE	Niger
NL	Netherlands
NO	Norway
NZ	New Zealand
PL	Poland
PT	Portugal
RO	Romania
RU	Russian Federation
SD	Sudan
SE	Sweden
SI	Slovenia
SK	Slovak Republic
SN	Senegal
TD	Chad
TG	Togo
UA	Ukraine
US	United States of America
UZ	Uzbekistan
VN	Viet Nam

EMISSION-TRANSMISSION IMAGING SYSTEM USING SINGLE ENERGY AND DUAL ENERGY TRANSMISSION AND RADIONUCLIDE EMISSION DATA

GOVERNMENT SUPPORT

The Government has rights in this invention pursuant to Grant No. DK-39964 awarded by the National Institutes of Health.

BACKGROUND OF THE INVENTION

This invention relates generally to x-ray transmission and radionuclide emission imaging systems. In a primary application the invention relates to a diagnostic imaging system where x-ray transmission data are used to derive material properties of the object imaged, which properties are then used directly to correct radionuclide emission data obtained from the same object using the same imaging system, herein referred to as X-SPECT.

Diagnostic imaging techniques can image both anatomical structure and physiological function of patients in whom the physician wishes to diagnose disease or follow treatment. In clinical settings, most of these diagnostic imaging techniques -- including conventional film radiography, MRI, and CT -- predominantly image structure rather than function. Unlike these anatomical imaging methodologies, *in vivo* measurement of tissue metabolism, perfusion, and biochemical processes is best performed with emission radionuclide-tracer techniques. In these techniques, a radionuclide or a compound labeled with a radionuclide is injected into a subject. The radiolabelled material concentrates in an organ or lesion of interest, and can show a concentration defect. At a prescribed time following injection, the pattern of concentration of the radiolabelled material is imaged by a rectilinear scanner, scintillation camera, single-photon emission computed tomography (SPECT) system, or positron emission tomography (PET) system. Applications of radionuclide imaging include quantitation of tissue metabolism and blood flow, evaluation of coronary artery disease, tumor and organ localization and volume determination, quantitation of receptor binding, measurement of brain perfusion, and liver imaging.

The radionuclide imaging procedure requires a means to define the path along which the emitted gamma-ray travels before striking the detector of the imaging system. The path can be a vector path, a line, narrow fan, or a narrow cone as defined by the detector or collimator. In rectilinear scanners, scintillation cameras, and SPECT systems, a collimator (typically made of lead or other high-atomic number material) is interposed between the object and the detector to define the gamma-ray path. In PET, the unique characteristics of positron annihilation radiation are coupled with electronic circuitry to define the vector path. In all cases, the only information obtained when a gamma-ray strikes the detector is the fact that the photon originated somewhere within the object along the vector path projected back from the detector. For projection imaging systems, a two-dimensional image is formed with the intensity of each picture element, or pixel, proportional to the number of photons striking the detector at that position. In SPECT or PET, the vector paths are determined for multiple projection positions, or views, of the object, and cross-sectional or tomographic images are reconstructed of the object using standard algorithms. Again, the intensity assigned to each vector path is proportional to the number of photons striking the detector originating along the path, and the intensity of each pixel in the reconstructed image is related to these vector path intensities obtained at multiple views.

In radionuclide imaging, it is desirable to obtain absolute values for radionuclide concentrations (or radionuclide uptake) at each point in the image. Attenuation of the emitted photons within the object, before they reach the detector, is a function of the energy of the photons and the exact composition of the material through which the photons pass to reach the detector.

Photons emitted deeper within the object have a higher probability of attenuation than those emitted near the surface. In addition, the composition of the material (in terms of effective atomic number Z and electron density) affects the attenuation, with more attenuation if the path passes through high-Z or high-density regions. Thus, in order to calculate absolute uptake or concentration of a radionuclide in a region of an object, it is required that the path length of each type of material or tissue (or effective-Z and electron density path lengths) be known for each vector. Attenuation corrections for emitted photons are made from this knowledge, allowing accurate concentration values to be obtained.

The full clinical potential of radionuclide imaging has been seriously hindered by some important limitations. The spatial resolution and photon statistical limitations of radionuclide imaging frustrate accurate anatomical localization and hinder quantitation of the radionuclide distribution. Photon attenuation has been identified by the American Heart Association and leading nuclear cardiologists as a major deficiency in diagnosis of heart disease with SPECT, and is a major source of error in the measurement of tumor metabolism using radionuclide techniques. Quantitation is further complicated by the need for scatter compensation for imaging with both single-photon and positron-emitting radionuclides.

A number of researchers have shown that many of these limitations can be overcome through use of emission-transmission imaging techniques which combine anatomical (structural) information from transmission images with physiological (functional) information from radionuclide emission images. By correlating the emission and transmission images, the observer can more easily identify and delineate the location of radionuclide uptake. In addition, the quantitative accuracy of measurement of radionuclide uptake can be improved through use of iterative reconstruction methods which can account for these errors and improve the radionuclide images.

Currently existing medical imaging instrumentation has been designed for either emission or transmission imaging, but not both, and attempts to perform both compromise one or both of the data sets. In addition, as currently implemented, iterative reconstruction algorithms are too slow to converge and therefore impede the flow of information in a hospital setting. Virtually all clinical tomographic systems use analytic rather than iterative reconstruction algorithms which, unlike iterative reconstruction techniques, have the major advantage that the image reconstruction process can occur concurrently with the acquisition of the image data. The efficiency of analytic approaches is compromised by their inability to account for the quantitative errors of photon attenuation, scatter radiation, and spatial resolution losses mentioned above.

The prior art in this field includes several different approaches to localize and quantify the uptake of radionuclides in the human body. One approach uses stereotactic techniques or computer processing methods to correlate functional information from SPECT or PET images with morphologic information from magnetic resonance imaging (MRI) or CT. This technique has the advantage that it can be applied retrospectively without acquiring new image data from the patient. However, these approaches are computationally intensive, require that the patient be scanned separately on two systems, and have only been successful in the head where the skull limits motion of internal anatomical structures.

A second set of prior art describes instrumentation used to detect emission and transmission data using instruments with single or multiple detectors. Several investigators have acquired both the emission and transmission images, with a radionuclide point, line, or sheet used as the transmission source which is placed on the opposite side of the body from the scintillation camera. This approach has been applied more recently using SPECT. Studies have shown that this technique is capable of producing adequate attenuation maps for attenuation correction to improve quantitation of radionuclide uptake, and that some modest anatomical localization of the radionuclide distribution is also possible.

An alternative approach uses specially-designed instruments for emission-transmission imaging. For example, Kaplan (International Patent Application No. PCT/US90/03722) describes an emission-transmission system in which the emission and transmission data are acquired with the same detector (single or multiple heads). An alternative emission-transmission imaging system (disclosed in SU-1405-819-A) uses x-ray transmission data and two detectors for determining the direction of the photons to improve detection efficiency. However, an exact method of correcting emission data based on transmission data is not described by either Kaplan or in SU-1405-819-A.

Other prior art notes that the map of attenuation coefficients required for the attenuation correction procedure can be obtained from a separate x-ray transmission CT scan of the patient, although a specific method of generating an attenuation map at the photon energy of the radionuclide source is not known. Specific techniques to determine the attenuation map of the patient from single-energy transmission measurement using radionuclide or x-ray sources have been described which are limited to sources emitting monoenergetic (line) spectra rather than broad spectra such as those typically obtained from an x-ray source.

Specific algorithms for correcting beam-hardening artifacts use single-energy x-ray data and dual-energy x-ray data. As used herein, the term "single-energy x-ray" describes methods in which an image is generated by integrating the x-ray signal over a single range of photon energies. As used herein, the term "dual-energy x-ray" describes methods in which two images are generated by integrating the signal over two different photon energy ranges. Thus, either "single-energy x-ray" or "dual-energy x-ray" includes methods in which the x-ray source emits an x-ray beam having either a narrow of broad spectrum of energies. Algorithms for correcting beam-hardening artifacts by using basis-material measurements derived from single-energy or dual-energy x-ray data have been presented but without describing how these measurements can be applied to correction of radionuclide data. Especially for single-energy measurements, the correction techniques associated therewith are principally directed at the removal of beam-hardening streaks and nonuniformities which disturb the qualitative evaluation of images produced with CT.

A key element has been the combination of the emission and transmission data in a reconstruction algorithm which corrects the radionuclide distribution for photon attenuation. Several authors have described analytic algorithms such as filtered backprojection in which the radionuclide data is modified using an attenuation map to correct for attenuation errors. Among their advantages, these analytic algorithms are fast and require only a single step to reconstruct the radionuclide distribution. However, they are inexact and utilize a uniform attenuation map in which the value of the attenuation coefficient is assumed to be constant across the patient. Other reconstruction algorithms are iterative and use an exact attenuation map and the radionuclide projection data to estimate the radionuclide distribution across the patient. Maximum likelihood estimation is one statistical method that can be used for image reconstruction. A maximum likelihood estimator appropriate for radionuclide tomography based on an iterative expectation maximization algorithm (ML-EM) has been described. The ML-EM algorithm is easy to implement, accounts for the Poisson nature of the photon counting process inherent with radionuclide imaging, and it produces better images than filtered backprojection. In addition, ML-EM algorithms can incorporate physical phenomena associated with radionuclide tomography, such as photon attenuation and scatter, detection efficiency, and geometric aspects of the imaging process. Iterative weighted least squares/conjugate gradient (WLS/CG) methods have also been proposed and used for radionuclide tomography. Overall, WLS/CG reconstruction algorithms converge faster than ML-EM procedures, while still incorporating the statistical nature of radionuclide imaging, and permit compensation for photon attenuation and scatter, detection efficiency and geometric response. Iterative algorithms have been successfully used for both SPECT and PET imaging.

The major disadvantage of iterative algorithms is their computational burden. Iterative algorithms are iterative procedures and are started with an initial image estimate that either corresponds to a constant radionuclide density throughout the image plane to be reconstructed or corresponds to constant density throughout the highly sampled "reconstruction circle" and zero outside this region. This estimate is unlikely to be representative of the actual distribution of radionuclide in a patient, and a large fraction of the total iterations required to generate useful images may be necessary to reveal the real qualitative structure of the radionuclide distribution. Thus, these algorithms often require 30 to 50 iterations to yield visually acceptable images, and possibly several hundred iterations to generate quantitatively accurate reconstructions.

It also is possible to use filtered backprojection to produce initial image estimates for iterative reconstruction algorithms. Filtered backprojection algorithms can operate concurrently with the emission data acquisition, and they are the method currently used for most clinical radionuclide imaging systems due to their efficiency and ability to produce useful images. Unfortunately it is generally not possible to modify filtered backprojection algorithms to accurately account for details of the collimator geometry, or for the effects of scatter, especially in regions where there are large inhomogeneities in these properties, or details of the collimator geometry. Therefore, this approach can speed up iterative techniques slightly, although the improvement in convergence speed has not been dramatic. Thus, many investigators have pursued various methods of speeding the convergence of ML-EM algorithms or reducing the time required per iteration. Methods include exploiting the symmetry of the imaging system, multigrid approaches, high frequency enhanced filtered iterative reconstruction, expectation maximization search (EMS) algorithms, rescaled gradient procedures, vector-extrapolated maximum likelihood algorithms, and hybrid maximum likelihood/weighted least squares (ML/WLS) algorithms. However, all iterative reconstruction methods require significantly more computer time than filtered backprojection algorithms to generate useful images. The iterative ML-EM and WLS/CG algorithms mentioned above assume complete sets of radionuclide projection data exists prior to commencement of the reconstruction procedure. The requirement to acquire complete sets of projection data is especially important in radionuclide system because clinical emission imaging systems typically require several minutes to acquire projection data, making iterative reconstruction techniques impractical.

SUMMARY OF THE INVENTION

The present invention is a system for acquiring correlated transmission and emission images with a dedicated imaging instrument, and includes the algorithms to process the emission and transmission data to calculate the radionuclide concentrations in the anatomical regions being imaged. A radiation detector is provided to record radionuclide images like a standard radionuclide imaging system. In addition, the system contains a transmission source and detector for acquisition of transmission images from which the anatomy of the body can be determined. The transmission source may be either a radionuclide or an x-ray tube or other radiation generating device. The transmission detector may be the same detector or a different detector from the radionuclide detector. In addition, a method is provided to maintain the relative spatial locations between the emission and transmission data sets. This can be performed by placing a localizing apparatus on the patient which is scanned concurrently with the patient. Alternatively, because the emission and transmission detectors are supported on a common gantry or embodied in a single detector, it is possible to perform calibration scans on a phantom prior to acquisition of the patients from which the emission and transmission data can be registered. As defined herein, the concept of single imaging system includes those embodiments in which the emission and transmission detectors are mounted on separate but adjacent gantries which share a common patient table. This will allow the patient to be translated from one imaging system to the other without having the patient move relative to the patient-support of the common table.

Both the emission detector and the transmission detector are electronically connected to data acquisition electronics which receive the detector signals and generate signals representative of the radiation striking the detector. Typically, the detector signals are digitized and stored in a computer as projection data showing the emission and transmission radiation signals recorded from the patient. From the transmission data, the computer uses a tomographic reconstruction algorithm to calculate an attenuation map which shows the distribution of attenuation coefficients at each point across the volume imaged in the patient.

Because the emission and transmission data are registered spatially, the attenuation map can be used as input data which is used in the reconstruction of the radionuclide data. In this process, the attenuation map is used to correct the radionuclide projection for absorption by overlying tissue and is necessary for quantitative accurate calculations of the radionuclide concentrations within the patient. Typically, this is performed with an iterative reconstruction algorithm which also can correct for other physical perturbations such as photon-statistical noise, scattered radiation, and partial-volume effects. The transmission image also can be used as *a priori* information in Bayesian reconstruction algorithms to improve anatomical definition in the radionuclide image.

For visual evaluation, color-mapped radionuclide emission data can be superimposed on high-resolution transmission image in order to correlate physiological information with structural information. The system allows the operator to define a region-of-interest on a correlated transmission image which has better statistics and spatial resolution than the radionuclide image. Thus, the inherent features of the emission-transmission system can improve the localization, accuracy, and precision of *in vivo* radionuclide measurements used to assess a patient's physiological status. Potential applications of emission-transmission imaging include tumor and organ localization and volume determination, myocardial perfusion, quantitation of receptor binding, measurement of brain perfusion, and liver imaging.

The invention and objects and features thereof will be more readily apparent from the following detailed description of illustrative embodiments and appended claims when taken with the drawings.

BRIEF DESCRIPTION OF THE DRAWINGS

Figs. 1A, 1B, 1C, and 1D are isometric views of hardware of a system in accordance with four embodiments of the invention.

Fig. 2 is a flow diagram illustrating signal processing in the system of Fig. 1.

Figs. 3A-3C are schematics of detectors in the system of Fig. 1.

Fig. 4 is a schematic of a triple mode detector circuit for use in the system of Fig. 1.

Fig. 5 is a flow chart of a beam-hardening correction algorithm in accordance with the invention.

Fig. 6A illustrates a CT method of obtaining an attenuation map using a calibration phantom, and Fig. 6B illustrates the correlation between CT numbers and attenuation coefficients for known material properties.

Figs. 7A and 7B are flow diagrams illustrating two methods of concurrent iterative reconstruction in accordance with the invention.

DETAILED DESCRIPTION OF ILLUSTRATIVE EMBODIMENTS

Figs. 1A and 1B are isometric views of two embodiments of the emission-transmission imaging system in accordance with the invention showing a radiation source 10, a transmission detector 12, and a radionuclide emission detector 14 all mounted to a gantry 16.

Fig. 2 illustrates the detection and processing of signals. Both the emission detector and transmission detector are electronically connected to data acquisition electronics with the transmission data used to generate an attenuation map which is then used to correct the emission data. In accordance with a feature of the invention, the emission image can be reconstructed using concurrent iterative reconstruction algorithms.

The system requires detectors for both the emission and transmission data. A single detector array can be used for both emission and transmission imaging, as shown in Figs. 1A and 1B. An alternative approach shown in Figs. 1C and 1D uses separate detector arrays for emission and transmission imaging. In Fig. 1A a two-dimensional transmission detector is used, while in Fig. 1B a one-dimensional transmission detector array is used.

One-dimensional detectors acquire images of a single plane in the patient during a single tomographic scan, while two-dimensional detector arrays acquire images from an entire volume. However, the transmission detector can be designed to use a limited cone-beam or fan-beam geometry. For example, single-slice and spiral fan-beam geometries can be used while translating the object across the stationary x-ray fan-beam. These approaches have the disadvantage that a longer period of time is required to obtain the x-ray data, but have the advantages that this detector configuration are less expensive and have better scatter-rejection characteristics.

Conventional CT scanners typically use scintillation detectors coupled to photodiodes, which are operated in a current mode. Radionuclide imaging systems use scintillators such as sodium iodide or bismuth germinate (BGO) which are coupled to photomultiplier tubes or photodiodes. However, other detector technologies can be used for emission-transmission imaging. In the pulse-counting regime, semiconductor detectors can be used, including HPGe, cadmium telluride, zinc cadmium telluride, and mercuric iodide. Scintillation detectors also can be operated in a pulse-counting mode, but are impractical for x-ray transmission measurements due to their low count-rate capabilities. Similarly, multiwire proportional counters operate in a pulse-counting mode, but have inadequate count-rate capabilities and poor detection efficiencies for the x-ray energies used in the emission-transmission system. Among current-integrating systems, pressurized xenon ionization detectors have been used for x-ray CT but are difficult to manufacture and to operate as area detectors. Hydrogenated amorphous silicon (a-Si:H) plates are being investigated as two-dimensional radiation detectors which integrate the photodiode, capacitor, and FET switch on a single substrate. Image intensifiers are compatible with cone-beam x-ray geometries, but suffer from pin-cushion distortion and veiling glare which complicate quantitative measurements. In addition, they are relatively large, heavy, and expensive, especially in formats large enough for body scanning with a cone-beam geometry.

Scatter radiation contributes a significant error to quantitative transmission measurements in CT, and these errors are aggravated in a system using an area detector. Therefore, it is desirable but not essential that the transmission detector is operated with a collimator to reject scatter. In addition, scatter compensation algorithms can be applied to the transmission projection data before it is reconstructed using a tomographic algorithm. Radionuclide imaging devices typically are operated with energy discrimination which reduces the amount of scatter radiation in the recorded data. In addition, several scatter compensation algorithms have been developed to provide additional corrections for scattered radiation. In emission-transmission imaging, the radionuclide detector can receive large amounts of scattered radiation during acquisition of the x-ray transmission image. To avoid this source of error from affecting the radionuclide data, the emission and transmission projection data can be acquired sequentially rather than simultaneously. During acquisition of the x-ray transmission data by the transmission detector, the scintillation camera can be protected from turning these high photon fluxes using a lead-lined cover. Alternatively, the scintillation detector used for radionuclide imaging can be turned off during the transmission scan to protect the photomultiplier tubes from damage from the high photon fluxes. Scintillation detectors used for radionuclide imaging commonly are operated with photomultiplier tubes (PMT's), which can be damaged by high photon fluxes.

Compensating filters can be used to decrease dynamic range, and thereby improve both the scatter and signal-to-noise characteristics of the recorded transmission signal. Compensating filters also introduce spatially-dependent changes in x-ray beam-hardening, which can introduce errors into quantitative transmission measurements. As will be described herein below, accuracy errors contributed by beam-hardening artifacts are corrected using uniformity corrections as well as iterative correction techniques. Additional corrections are derived from the use of aggressive filtration of the x-ray beam to derive quasi-monoenergetic spectra. It also is possible to use dual-energy CT to derive attenuation maps of sufficient accuracy and precision for attenuation-correction of the radionuclide data.

Aggressive x-ray beam filtration also can be used to reduce errors in the x-ray transmission measurement which results from use of iodinated contrast media which have attenuation coefficients with a k-edge within the photon energy range used to acquire the transmission data. This nonlinearity introduces errors into calculation of the attenuation map from the beam-hardening correction described in this disclosure and can require that we can filter the x-ray beam so that its spectrum falls above the iodine k-edge to avoid these nonlinearities.

As noted above, the emission-transmission system can use either separate detectors or a single detector to record the emission and transmission data. The ideal implementation of this instrument is to use a single detector so that the emission and transmission data can be spatially registered, and potentially can be recorded simultaneously. However, the use of a single detector is complicated because differences in the acquisition requirements of the transmission and emission data are extreme. The transmission data are acquired with a point or line source, typically at high data rates, and do not require energy discrimination. Therefore, transmission CT scanners use detectors operated in the "current" or "integrating" mode, where the electronic circuitry attached to the detector reads the current produced by absorption of one or more photons in a unit of time (Fig. 3A). In comparison, radionuclide imaging typically is performed at low data rates and requires energy discrimination so that unscattered emission photons can be separated from those which are scattered within the body. Emission imaging devices therefore use detectors operated in the "pulse" or "counting" mode in which signals are generated for single photons and where the signal amplitude is proportional to the photon energy (Fig. 3B). Finally, when simultaneous emission-transmission imaging is performed, the circuitry must operate at high count rates (to accommodate the photon flux from the transmission source) but must operate in a "count" or "pulse" mode to allow discrimination of the emission and transmission photons, as well as discrimination of scattered and unscattered photons from the emission source (Fig. 3C). For example, the component values in Fig. 3 are chosen to illustrate these applications for a high-purity germanium detector element having a thickness of 6-mm and a surface area of 2-mm x 10-mm and with a charge collection time of 50 ns. In Fig. 3A, the feedback resistor and capacitor values are chosen to produce the largest usable signal from the amplifier which is compatible with the photon flux received and the charge-conversion characteristics of the detector. In Fig. 3B and Fig. 3C, the values of the feedback resistor and capacitor are selected to provide a time constant which is long in comparison to the charge-collection time of the detector. However, in Fig. 3B, the pulse-shaping time constants and number of integrators are chosen to maximize the signal-to-noise characteristics of the circuit which optimizes the energy resolution capabilities for photon-counting at low count rates. In comparison, in Fig. 3C, the pulse-shaping time constants are chosen to be consistent with the charge collection time of the detector to maximize count rate with moderate energy resolution.

One possible implementation involves a novel "triple-mode" electronic circuit for the detector readout shown in Fig. 4. The input amplifier can function in either charge-sensitive pulse mode or in current mode. This flexibility is achieved by using a variable feedback resistor which can be made larger for charge sensitive operation or smaller for current mode operation. In addition, the feedback capacitance is chosen such that it is suitable as an integrating capacitor for pulse-mode operation or as a compensating capacitor for current mode operation. Following the input amplifier, several pulse shaping stages are available in parallel; the desired stage can be switched in for a given application. Fast pulse shaping is available for high count rate applications (x-ray imaging), and slow pulse shaping is available for low count rates (radionuclide imaging). No pulse shaping is necessary in current mode. In brief, the triple mode electronics allow the detector to be read out in current mode, fast pulse mode, and slow pulse mode. The circuit can be assembled from discrete components, or can be fabricated as an application-specific integrated circuit in which the resistor is implemented by a MOSFET operated in the ohmic region.

As previously noted, the prior art has suggested that x-ray CT can be used to obtain attenuation maps but has not described specific procedures to do so. This procedure is complicated by x-ray beam hardening that introduces errors in the quantitation of attenuation coefficients obtained with this technique. These errors can be compensated by conventional beam-hardening correction algorithms that use a CT scan of a uniformity phantom having an appropriate diameter to normalize the CT scans of other objects. These uniformity correction coefficients are parameterized in a look-up table giving the normalization factor as a function of the diameter and distance from the rotational center of the object. This technique corrects "global" uniformity errors, but does not correct "local" beam-hardening errors between two heterogeneities (e.g., bones) in the reconstruction volume. Therefore, the imaging system in accordance with the invention uses techniques to correct beam-hardening errors contributed by soft-tissue, water, and bone within the scanned object.

A flow chart of one technique for calculating the attenuation map for x-ray measurements is shown in Fig. 5. The correction procedure uses calibration scan of a bidirectional step-wedge containing known thicknesses of aluminum and acrylic. The transmission data are approximated as

$$I_c = f(A_{ac}, A_{al}) \qquad \textbf{(1)}$$

where the measured calibration intensities I_c are represented as a function (e.g., polynomial) of the known material thicknesses (A_{ac},A_{al}) in the calibration phantom.

We then acquire projection data $p^{\cdot}$ of the object (*i.e.*, phantom or patient), from which we reconstruct a tomogram using filtered backprojection or other standard technique. We assume voxels with more attenuation than acrylic contain a homogeneous mixture of acrylic and aluminum, while those with less attenuation than acrylic contain a homogeneous mixture of acrylic and air. Based on the reconstructed attenuation coefficients, we assign a fractional contribution of acrylic (a_{ac}) and aluminum (a_{al}) to each voxel in the tomogram. (Because the attenuation properties of soft-tissue and bone can be approximated as linear combinations of acrylic and aluminum, each voxel could be equivalently expressed in terms of fractional weights of soft-tissue and bone.) The fractional weights are used as first estimates in the following iterative process to correct their values for beam-hardening.

In the iterative process, the n^{th} estimate of the basis set coefficients $(a_{ac}^{(n)}, a_{al}^{(n)})$ are projected to give the n^{th} estimate of the equivalent ray-sums $(A_{ac}^{(n)}, A_{al}^{(n)})$ of the two basis materials

$$A_{ac}^{(n)} = \int_L a_{ac}^{(n)}(x,y)\,ds \quad \text{and} \quad A_{al}^{(n)} = \int_L a_{al}^{(n)}(x,y)\,ds \qquad (2)$$

for each set of projection data. These values are used to obtain the n^{th} estimate the projected transmission values p_n from Eq. 1, so that

$$p_n = f(A_{ac}^{(n)}, A_{al}^{(n)}) \qquad (3)$$

Assuming the difference between p_n and the experimental projection data p is small, error estimates $(\Delta_{ac}^{(n)},\Delta_{al}^{(n)})$ for the ray-sums $(A_{ac}^{(n)},A_{al}^{(n)})$ can be determined from a first-order Taylor's series expansion of Eq. 1

$$p \approx f(A_{ac}^{(n)}, A_{al}^{(n)}) + \frac{\partial f}{\partial A_{ac}}\Big|_{(A_{ac}^{(n)},A_{al}^{(n)})} \Delta_{ac}^{(n)} + \frac{\partial f}{\partial A_{al}}\Big|_{(A_{ac}^{(n)},A_{al}^{(n)})} \Delta_{al}^{(n)} \qquad (4)$$

and a second arbitrary constraint, such as

$$\frac{\Delta_{al}^{(n)}}{\Delta_{ac}^{(n)}} = \frac{A_{al}^{(n)}}{A_{ac}^{(n)}} \qquad (5)$$

Corrected estimates of the n^{th} iterative ray-sums, $(A_{ac}^{(n)} + \Delta_{ac}^{(n)}, A_{al}^{(n)} + \Delta_{al}^{(n)})$ are determined for each experimentally measured projection, and the set backprojected to give the $(n+1)^{th}$ iterative estimate of the acrylic and aluminum densities for each voxel. This procedure is repeated until the acrylic and aluminum densities within each voxel are stable to within 0.5% (or other accuracy level) of the densities obtained on the previous iteration.

This iterative beam-hardening algorithm converges toward a pair of images describing the equivalent density contributions of the aluminum and acrylic basis materials for each voxel of the original uncorrected image. These values can be used to estimate the monoenergetic attenuation map used for attenuation correction of the radionuclide image. The attenuation map at the point (x,y) is calculated as

$$\mu(x,y;E) = a_{ac}(x,y)\,\mu_{ac}(E) + a_{al}(x,y)\,\mu_{al}(E) \qquad (6)$$

where E is chosen to be the photon energy of the radionuclide (*e.g.*, 140 keV for ^{99m}Tc, and where $\mu_{ac}(E)$ and $\mu_{al}(E)$ are the linear attenuation coefficients of acrylic and aluminum at the energy E. The resulting attenuation map then can be used as input data for the reconstruction of the radionuclide image. These data also can be analyzed directly for quantitative measurement of tissue components at each point in the image.

Other techniques can be used to obtain an accurate attenuation map for this application. One class of these techniques uses a calibration phantom which is scanned simultaneously rather than separately from the patient as illustrated in Fig 6A and 6B. The phantom includes distinct regions which contain materials similar in the x-ray attenuation properties to those found in the human body. After the patient and phantom are scanned, the image is read into a computer where the derived CT number from the various regions of the calibration phantom are related to their known material properties. The known material properties then can be correlated with the attenuation coefficients of these materials at the radionuclide energy, thereby giving an equation which transforms the measured CT numbers from the image to desired attenuation coefficients. In some cases, this relationship will be sufficient to generate the desired attenuation map. However, the existence of beam-hardening and other errors require that the calibration measurements be used to calculate material properties of the patient which are entered into an iterative correction algorithm such as that described above, which is used to generate an accurate attenuation map of the patient including corrections for beam-hardening errors.

In accordance with another feature of the invention, a new class of concurrent iterative reconstruction algorithms is provided. These "concurrent" algorithms reconstruct the image during (rather than after) acquisition of the radionuclide data, thereby speeding up the overall image reconstruction process. As with iterative reconstruction methods, the major motivation for using concurrent reconstruction algorithms is to account for physical effects so that qualitatively improved and quantitatively accurate images can be obtained. However, the concurrent iterative reconstruction algorithms process partial sets of projection data during the acquisition phase to dramatically reduce the elapsed time required to obtain and reconstruct the radionuclide image.

Two general approaches have been developed, which use only subsets of projections and which can be described in terms of the ML-EM algorithm as follows. From a numerical analysis perspective, the image reconstruction problem reduces to finding the global minimum (or maximum) of an "objective function" or "cost function." The objective function is constructed such that the image associated with the least (or greatest) cost is in some probabilistic sense "most" representative of the distribution of radionuclide within a patient. For ML-EM reconstruction algorithms, the goal of the reconstruction procedure can be stated as maximizing the following objective function:

$$O_{ML} = \sum_{d=1}^{N_d} \left[\sum_{b=1}^{N_b} \lambda_n(b)\, w(b,d) \; + D^*(d) \log\left(\sum_{b=1}^{N_b} \lambda_n(b)\, w(b,d) \right) \right] \quad (7)$$

In the above equation, λ_n is the n^{th} iterative estimate of the radionuclide distribution, D^* is the vector of measured counts for each detector in the imaging system, and the transition matrix w gives the probability of a photon emitted from pixel b being detected in detector d. The sum over d in Eq. 7 extends over all N_d detectors in the acquired radionuclide data, while the sum over b extends over all N_b pixels in the reconstructed radionuclide image. Physical aspects of the imaging process, including geometric response of the imaging system, and photon attenuation and scatter, are incorporated in the transition matrix, which includes information derived from the transmission image. The objective function for WLS/CG reconstruction algorithms is somewhat different, although the general goal of minimizing an objective function is identical to that of the ML-EM algorithm given in Eq. 7.

The objective functions for the concurrent algorithms have the same form as Eq. 7, however, the sum over detectors, d, does not include all N_d projections that are ultimately used to form the final image. This is a necessary requirement for these reconstruction methods to take place simultaneously with the acquisition of radionuclide projection data. For example, two approaches can be used to obtain the iterative image estimates, but differ in the manner used to generate subsets of projection data. The first approach for processing projection subsets, illustrated in Fig. 7A and referred to here as the method of "sequential subsets," will be started with a uniform image estimate and some minimum number of projections, N_{Min}, available during the radionuclide scan. Thus, the sum over detectors in the appropriate objective function contains N_{Min} terms. A WLS/CG or ML-EM type algorithm will then be used to generate the first iterative image estimate. After the first iteration is completed, any new projections available from the radionuclide imaging system will be incorporated in the projection subset, and the next iterative image estimate will be generated. This method of sequentially adding projections to the reconstruction subset is continued until all N_d projections are included in the reconstruction procedure. Additional iterations are performed with the complete set of projections until appropriate stopping conditions are satisfied.

The second method for processing the radionuclide projection data, illustrated in Fig. 7B and referred to here as the method of "independent subsets," again starts with a uniform image estimate and some minimum number of projections. A fixed number of iterations, N_{iter}, of a WLS/CG or ML-EM type algorithm is used to generate a "subimage" from this subset of projections. The next set of N_{Min} projections available from the radionuclide imaging system will then be reconstructed in a similar manner. This procedure is repeated until subimages have been generated for all N_d projections with each subimage reconstructed from N_{Min} projections, and in general each projection appears in one and only one subset. In addition, it is reasonable that N_{iter} should be chosen such that reconstruction of a subimage is completed just as the next subset of projections is available. The subimages are then combined to form an initial image estimate for the post acquisition iterative reconstruction routine with the following procedure. Each pixel in the combined image will be constructed from a weighted linear combination of pixels in the respective subsets. The weights are determined from the transition matrix w appearing in Eq. 7. First, let $p_i(b)$ be the probability that photons emitted from pixel b are detected in subset i. For example, this probability can be calculated as

$$p_i(b) = \sum_{d_i} w(b, d_i) \tag{8}$$

where the sum over d_i includes all projections in subset i. Pixel b in the iterative initial image estimate, λ_o, then may be described by

$$\lambda_0(b) = \frac{\sum_{i=1}^{N_i} p_i(b)\,\lambda_i(b)}{\sum_{i=1}^{N_s} p_i(b)} \tag{9}$$

where i is indexed over all N_s subimages, λ_i.

Although the concurrent image estimates will be of sufficient quality to be of limited clinical utility, generally additional processing is necessary. Therefore, the concurrent images will be used as initial image estimates with complete sets of projection data in conventional iterative reconstruction procedure. The concurrent image estimates will not be restricted to use the same underlying reconstruction method as is used in the post-acquisition reconstruction phase.

It has been assumed that angular views with the radionuclide imaging system are taken at consecutive angles, and projection subsets for the concurrent algorithms contain consecutive angular views. This is the logical sequence for acquiring data with a single detector array. However, the imaging system can have two or three radionuclide detector arrays, providing projections corresponding to vastly different angular views of the patient simultaneously. This reduces the total scan time, and will improve the convergence rate of concurrent algorithms when projection subsets are constructed from data with significantly varying angles. In the preceding discussion, we have described how these concurrent techniques can be applied to the tomographic reconstruction of radionuclide images. However, as used herein, the terms "concurrent iterative reconstruction" and "concurrent reconstruction" include those applications in which iterative reconstruction algorithms include *a priori* information in the reconstruction of either emission or transmission data. In the case of emission imaging, the *a priori* information can include an attenuation map, information about scattered radiation, corrections for partial-volume effects derived from the transmission image. In the case of emission or transmission imaging, the *a priori* information can include a description of spatial resolution loss due to the geometrical characteristics of the system or the collimator.

Thus, while the invention has been described with reference to illustrative embodiments, the description is illustrative of the invention and is not to be construed as limiting the invention. Various modifications and applications may occur to those skilled in the art without departing from the true spirit and scope of the invention as defined by the appended claims.

WHAT IS CLAIMED IS:

1. An emission-transmission imaging system comprising

a) A radiation source for emitting a photon spectrum,

b) detector means for selectively detecting photons corresponding to said photon spectrum and photons corresponding to radionuclide emission,

c) means for positioning said radiation source facing said detector means with an object positionable therebetween, said object having a radionuclide therein,

d) data acquisition means connected with said detector means for receiving transmission signals from said detector means representative of said detected photon spectrum photons and radionuclide signals representative of detected radionuclide emission signals,

e) computer means for receiving and processing said transmission signals and developing an attenuation map for photons, said computer means receiving and processing said radionuclide signals using said attenuation map for attenuation correction and producing image signals of distribution of a radionuclide in an object positioned between said radiation source and said detector means, and

f) display means responsive to said image signals.

2. The emission-transmission imaging system as defined by claim 1 wherein said computer means processes said transmission signals by reconstructing an image of at least one slice through an object using computed tomography (CT) attenuation coefficients developed from said photon signals.

3. The emission-transmission imaging system as defined by claim 2 wherein said computer means processes said radionuclide signals using said attenuation map to correct for at least one of photon attenuation, scattered

radiation, and partial volume effects.

4. The emission-transmission imaging system as defined by claim 3 wherein said radiation source transmits single energy photons.

5. The emission-transmission imaging system as defined by claim 4 wherein said computer means receives and processes transmission signals from said detector means representative of a detected photon spectrum passed through a phantom for providing calibration data used in developing said attenuation map.

6. The emission-transmission imaging system as defined by claim 5 wherein said computer means iteratively processes said transmission signals and said radionuclide signals to reconstruct image signals of radionuclide distribution.

7. The emission-transmission imaging system as defined by claim 6 wherein said computer means uses subsets of complete radionuclide signals to reconstruct image subsets of radionuclide distribution which are combined to produce said image signals.

8. The emission-transmission imaging system as defined by claim 7 wherein said computer means reconstructs said image subsets concurrently with the acquisition of said radionuclide signals.

9. The emission-transmission imaging system as defined by claim 8 wherein said data acquisition means includes pulse counting circuitry operable at low count rates and high energy resolution for said radionuclide emission detection, pulse counting circuitry operable at high count rates and moderate energy resolution for simultaneous radionuclide emission and transmission detection, and current mode circuitry operable at very high

count rates without energy resolution for transmission detection.

10. The emission-transmission imaging system as defined by claim 9 wherein said data acquisition means includes means for switching said pulse counting circuitry.

11. The emission-transmission imaging system as defined by claim 1 wherein said data acquisition means includes pulse counting circuitry operable at low count rates and high energy resolution for said radionuclide emission detection, pulse counting circuitry operable at high count rates and moderate energy resolution for simultaneous radionuclide emission and transmission detection, and current mode circuitry operable at very high count rates without energy resolution for transmission detection.

12. The emission-transmission imaging system as defined by claim 11 wherein said data acquisition means includes means for switching said pulse counting circuitry.

13. The emission-transmission imaging system as defined by claim 1 wherein said radiation source is an x-ray source for emitting x-rays.

14. The emission-transmission imaging system as defined by claim 13 wherein said x-ray source transmits single energy x-rays.

15. The emission-transmission imaging system as defined by claim 13 wherein said computer means receives and processes x-ray signals from said detector means representative of detected x-ray spectrum photons passed through a phantom for providing calibration data used in developing said attenuation map.

16. The emission-transmission imaging system as defined by claim 1 wherein said computer means iteratively processes said transmission signals and said radionuclide signals to reconstruct image signals of radionuclide distribution.

17. The emission-transmission imaging system as defined by claim 16 wherein said computer means uses subsets of complete radionuclide signals to reconstruct image subsets of radionuclide distribution which are combined to produce said image signals.

18. The emission-transmission imaging system as defined by claim 17 wherein said computer means reconstructs said image subsets concurrently with the acquisition of said radionuclide signals.

19. The emission-transmission imaging system as defined by claim 1 wherein said detector means comprises a single detector for photons.

20. The emission-transmission imaging system as defined by claim 1 wherein said detector means includes a first detector for photons from said radiation source and a second detector for photons from said radionuclide.

21. The emission-transmission imaging system as defined by claim 1 wherein said radiation source comprises a radionuclide source.

22. A method of computed tomography (CT) image reconstruction comprising the steps of

a) directing photons through an object to be imaged,

b) detecting photons after passing through the object,

c) generating electrical signals indicative of detected photons,

d) modifying said electrical signals using parameters of the imaging system and attenuation effects of the object, and

e) reconstructing a CT image using subsets of said electrical signals as modified to reconstruct image subsets.

23. The method as defined by claim 22 wherein step e) occurs concurrently with steps b), c), and d).

24. The method as defined by claim 22 wherein step e) occurs after steps b), c), and d) are completed.

25. The method as defined by claim 22 wherein step a) includes use of a radionuclide source.

26. The method as defined by claim 22 wherein step a) includes use of an x-ray source.

27. The method as defined by claim 22 wherein step d) uses *a priori* knowledge of said parameters.

28. A method of forming an emission image from a radionuclide source in an object comprising

a) transmitting photons through said object,

b) detecting photons transmitted through said object and photons from the radionuclide source,

c) generating transmission signals based on detected photons transmitted through said object and emission signals based on detected photons from the radionuclide source,

d) processing said transmission signals to develop an attenuation map for photons

e) processing said emission signals using said attenuation map for attenuation connection, and

f) generating image signals using processed emission signals from step e).

29. The method as defined by claim 28 wherein steps d), e), and f) are repeated iteratively.

30. The method as defined by claim 29 wherein step f) includes generating image subsets using subsets of said transmission signals and subsets of said emission signals.

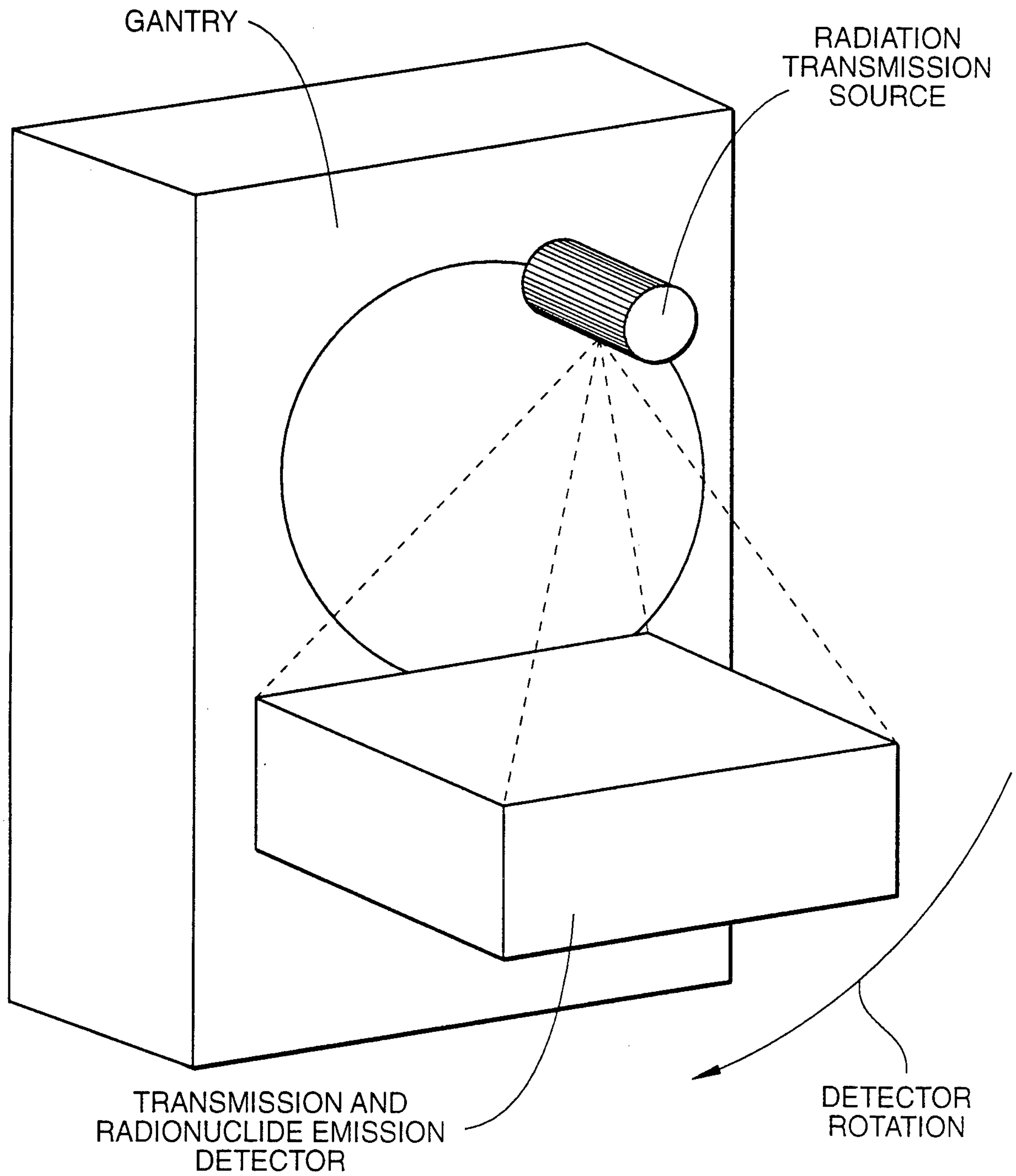
GANTRY
RADIATION TRANSMISSION SOURCE
TRANSMISSION AND RADIONUCLIDE EMISSION DETECTOR
DETECTOR ROTATION

FIG._1A

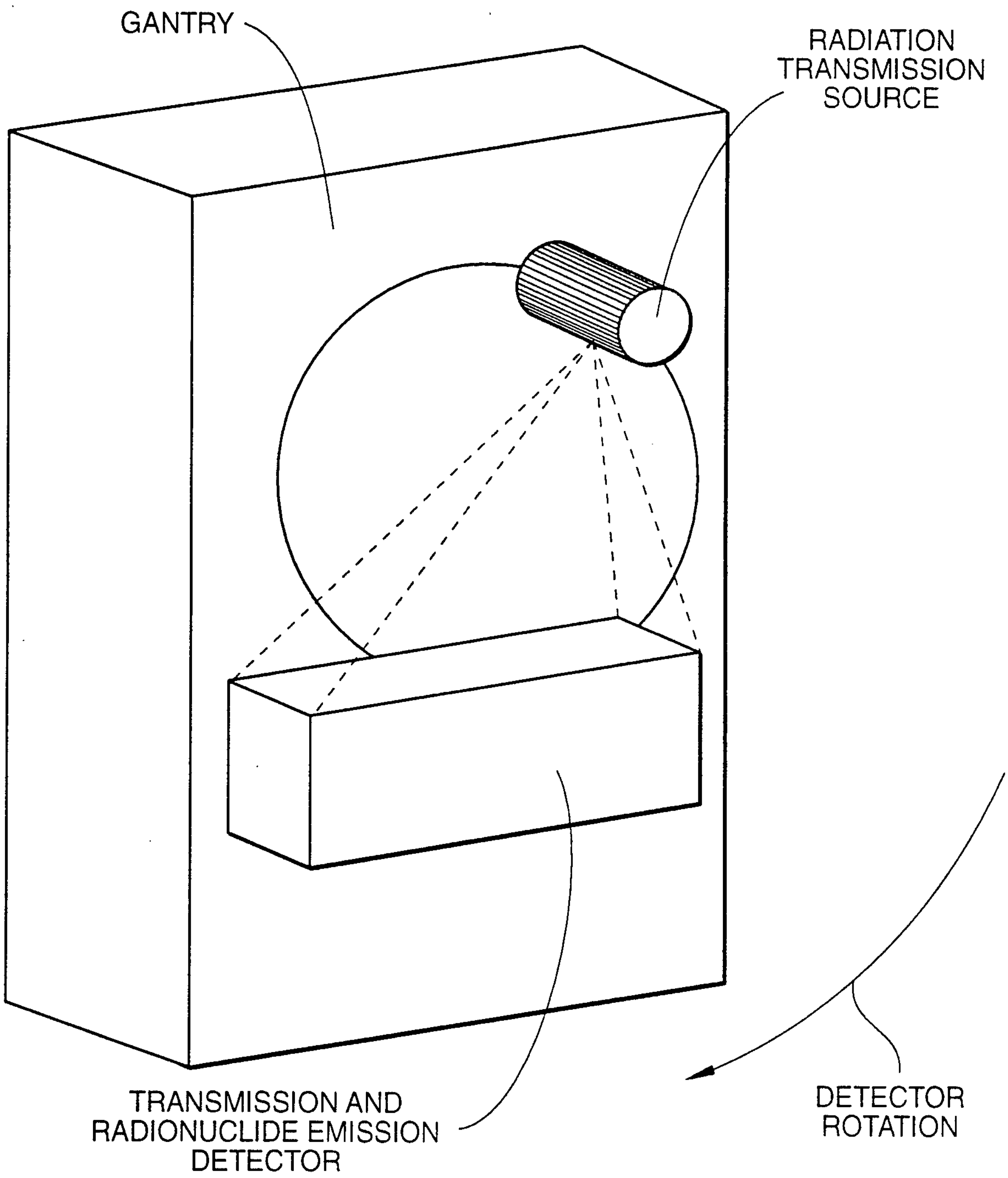
GANTRY
RADIATION TRANSMISSION SOURCE
TRANSMISSION AND RADIONUCLIDE EMISSION DETECTOR
DETECTOR ROTATION

FIG._1B

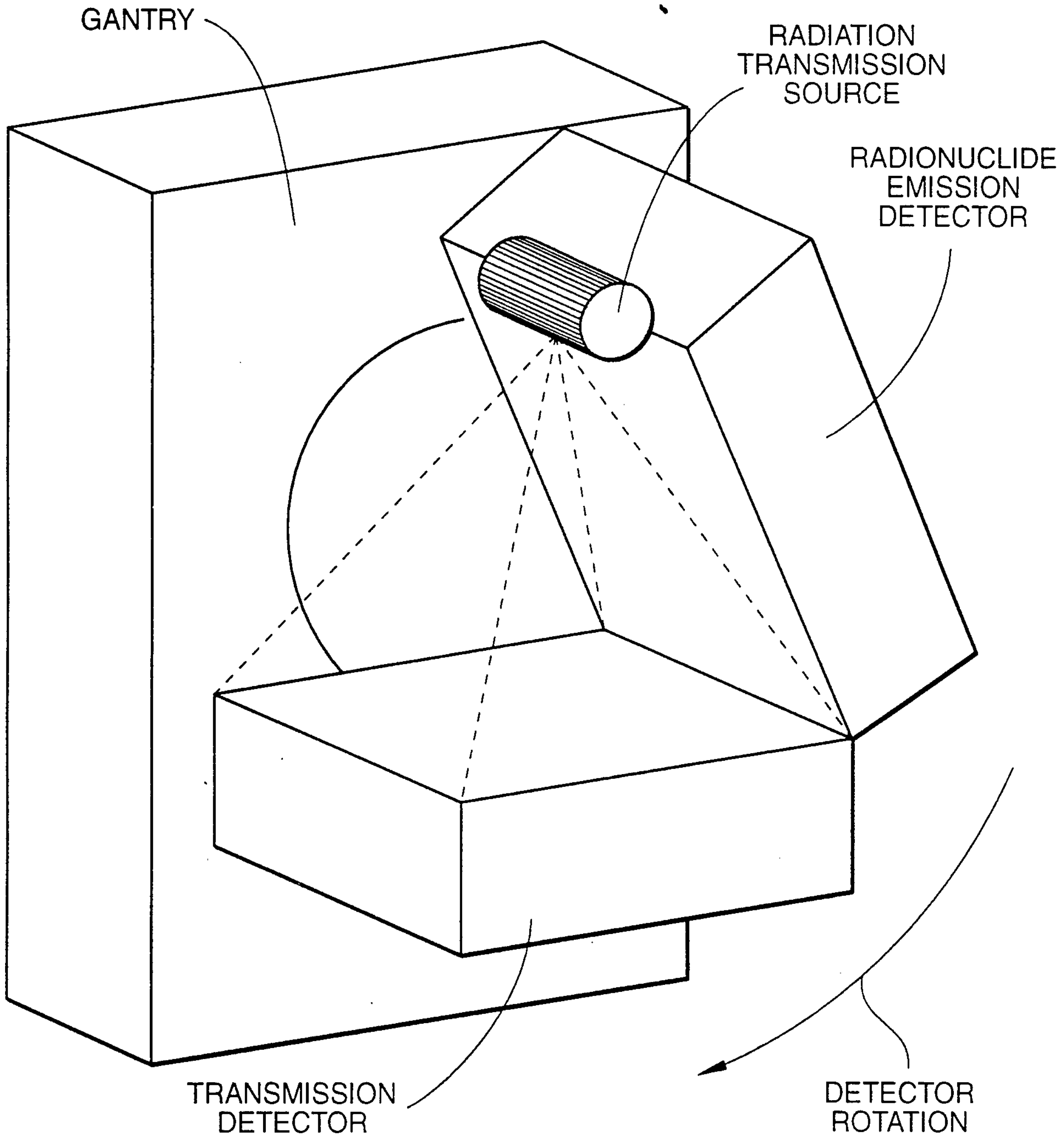
GANTRY
RADIATION TRANSMISSION SOURCE
RADIONUCLIDE EMISSION DETECTOR
TRANSMISSION DETECTOR
DETECTOR ROTATION

FIG._1C

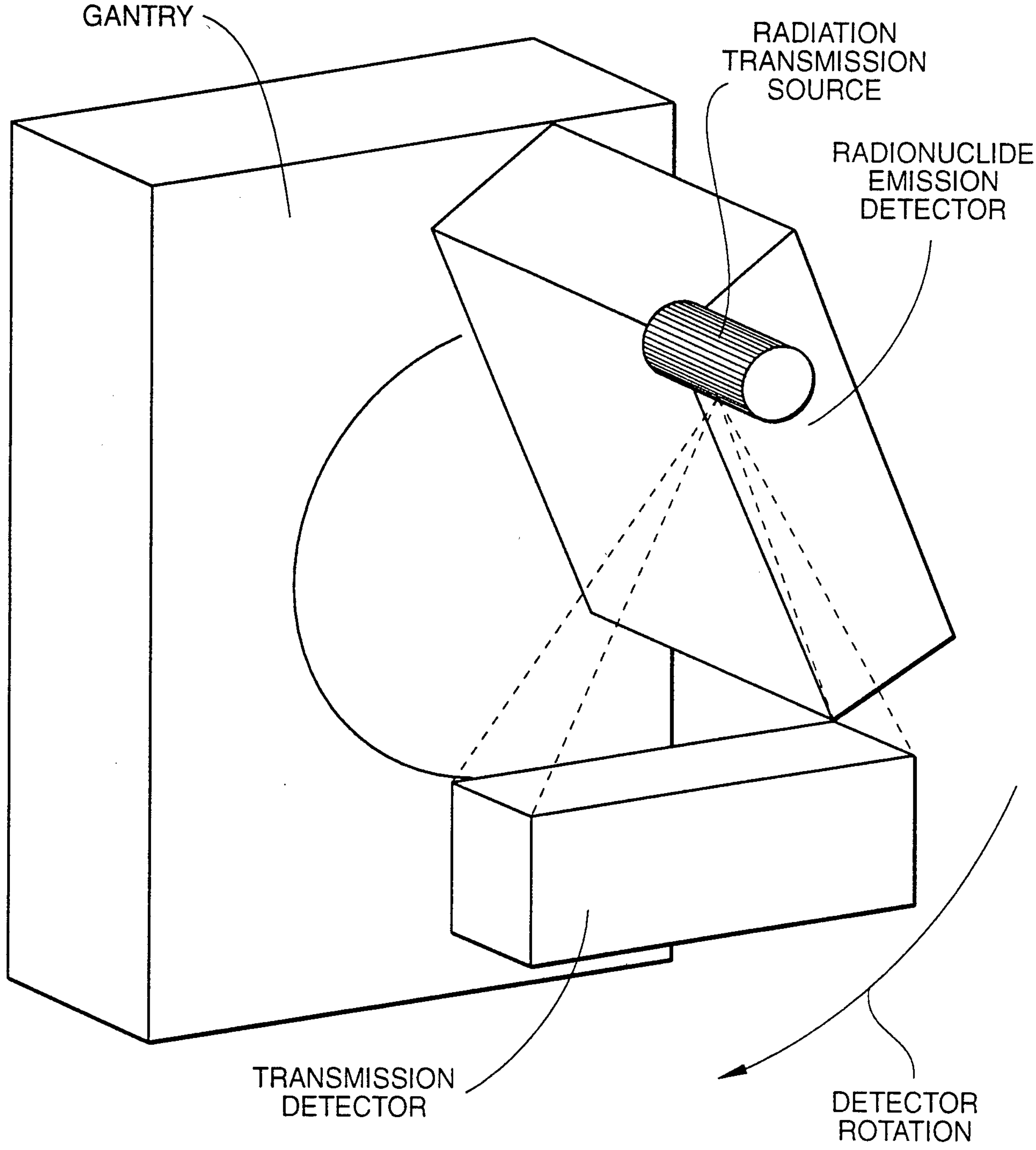
GANTRY
RADIATION TRANSMISSION SOURCE
RADIONUCLIDE EMISSION DETECTOR
TRANSMISSION DETECTOR
DETECTOR ROTATION

FIG._1D

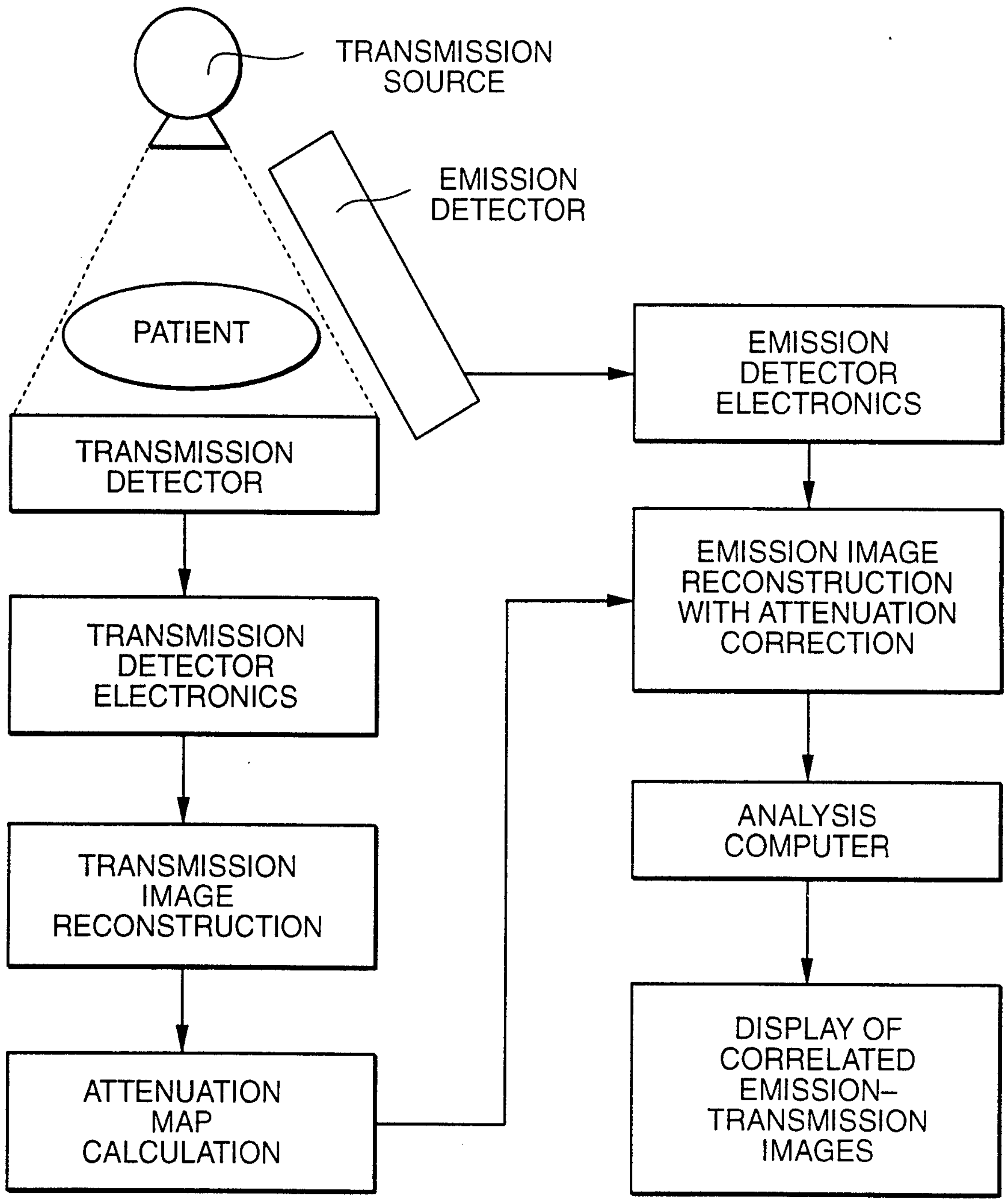
TRANSMISSION SOURCE
EMISSION DETECTOR
PATIENT
TRANSMISSION DETECTOR
TRANSMISSION DETECTOR ELECTRONICS
TRANSMISSION IMAGE RECONSTRUCTION
ATTENUATION MAP CALCULATION
EMISSION DETECTOR ELECTRONICS
EMISSION IMAGE RECONSTRUCTION WITH ATTENUATION CORRECTION
ANALYSIS COMPUTER
DISPLAY OF CORRELATED EMISSION–TRANSMISSION IMAGES

FIG._2

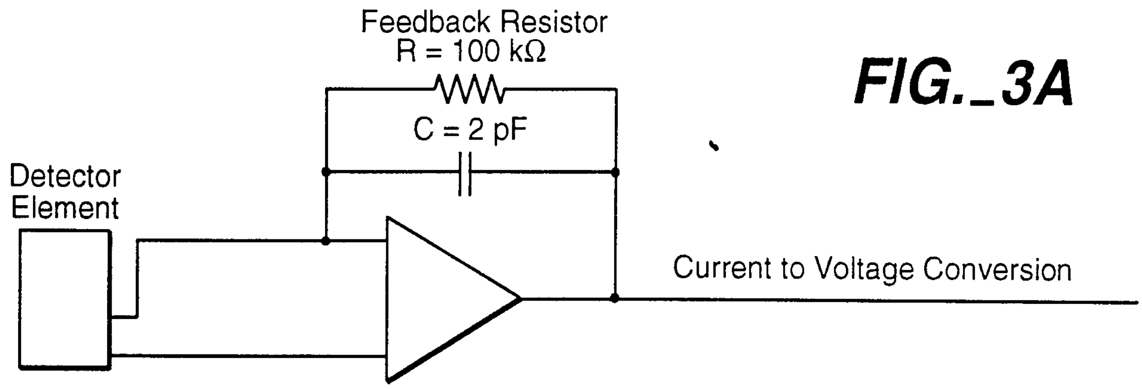

FIG._3A

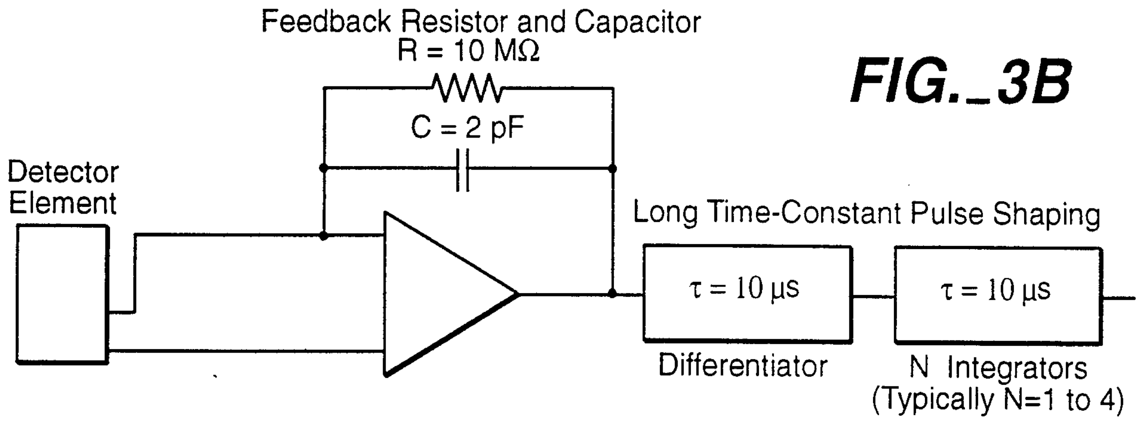

FIG._3B

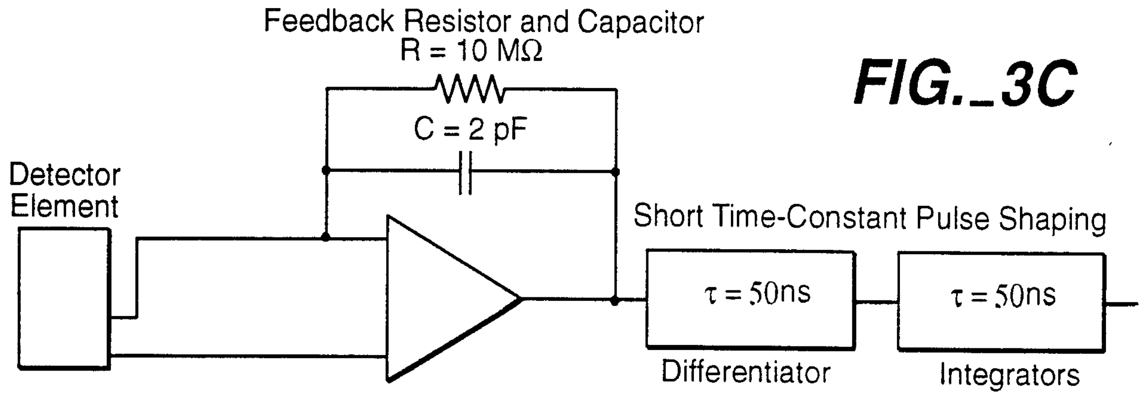

FIG._3C

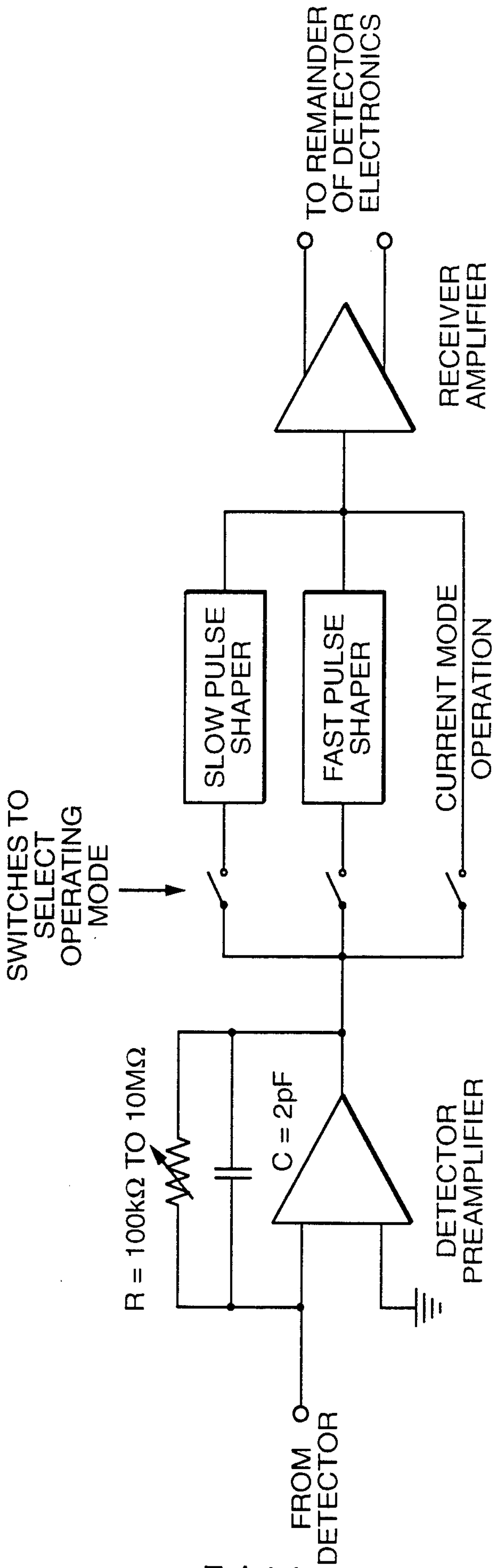
TO REMAINDER
OF DETECTOR
ELECTRONICS
RECEIVER
AMPLIFIER
SLOW PULSE
SHAPER
FAST PULSE
SHAPER
CURRENT MODE
OPERATION
SWITCHES TO
SELECT
OPERATING
MODE
R = 100kΩ TO 10MΩ
C = 2pF
DETECTOR
PREAMPLIFIER
FROM
DETECTOR

FIG._4

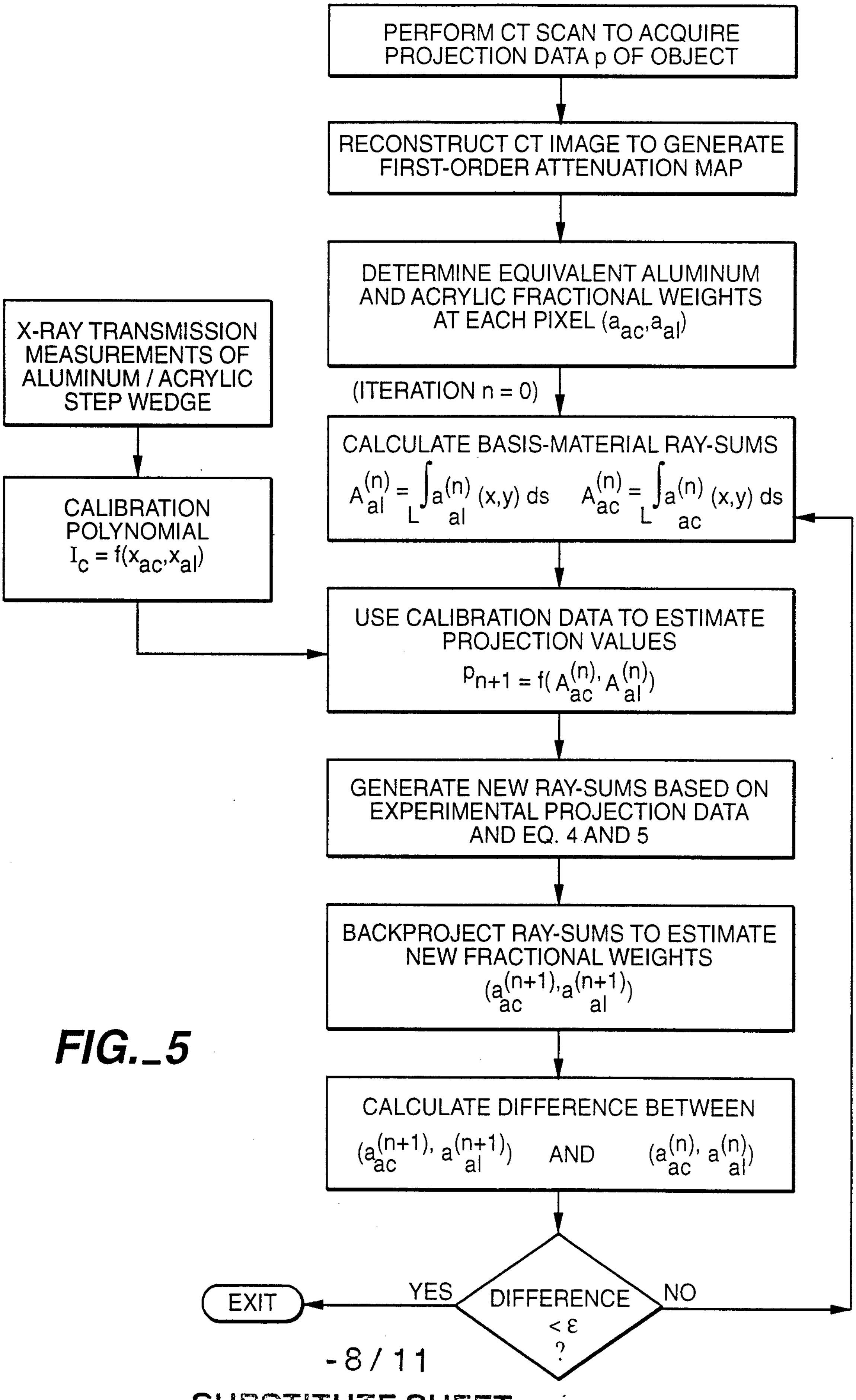
PERFORM CT SCAN TO ACQUIRE PROJECTION DATA p OF OBJECT
RECONSTRUCT CT IMAGE TO GENERATE FIRST-ORDER ATTENUATION MAP
DETERMINE EQUIVALENT ALUMINUM AND ACRYLIC FRACTIONAL WEIGHTS AT EACH PIXEL (a_{ac}, a_{al})
X-RAY TRANSMISSION MEASUREMENTS OF ALUMINUM / ACRYLIC STEP WEDGE
(ITERATION n = 0)
CALIBRATION POLYNOMIAL $I_c = f(x_{ac}, x_{al})$
CALCULATE BASIS-MATERIAL RAY-SUMS
$A_{al}^{(n)} = \int_L a_{al}^{(n)}(x,y)\,ds$ $A_{ac}^{(n)} = \int_L a_{ac}^{(n)}(x,y)\,ds$
USE CALIBRATION DATA TO ESTIMATE PROJECTION VALUES
$p_{n+1} = f(A_{ac}^{(n)}, A_{al}^{(n)})$
GENERATE NEW RAY-SUMS BASED ON EXPERIMENTAL PROJECTION DATA AND EQ. 4 AND 5
BACKPROJECT RAY-SUMS TO ESTIMATE NEW FRACTIONAL WEIGHTS
$(a_{ac}^{(n+1)}, a_{al}^{(n+1)})$
CALCULATE DIFFERENCE BETWEEN
$(a_{ac}^{(n+1)}, a_{al}^{(n+1)})$ AND $(a_{ac}^{(n)}, a_{al}^{(n)})$
DIFFERENCE $< \varepsilon$?
YES
NO
EXIT

FIG._5

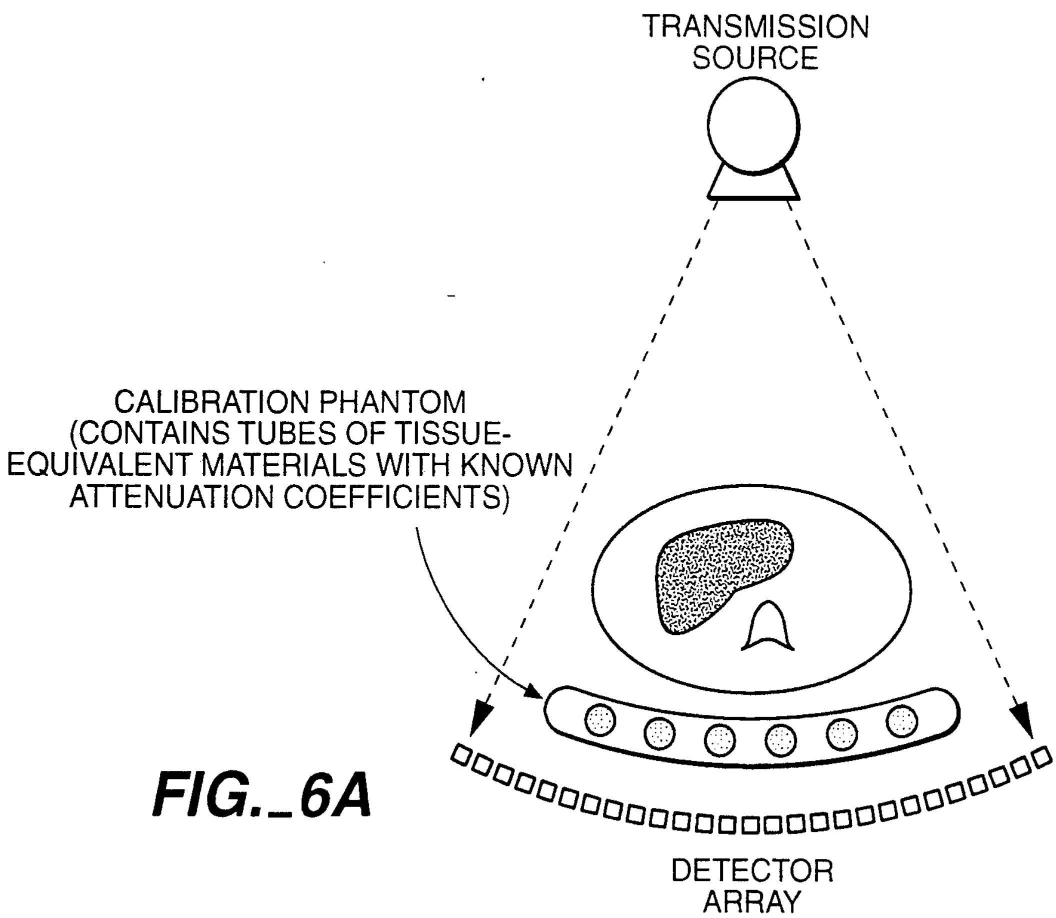
TRANSMISSION
SOURCE
CALIBRATION PHANTOM
(CONTAINS TUBES OF TISSUE-
EQUIVALENT MATERIALS WITH KNOWN
ATTENUATION COEFFICIENTS)
DETECTOR
ARRAY

FIG._6A

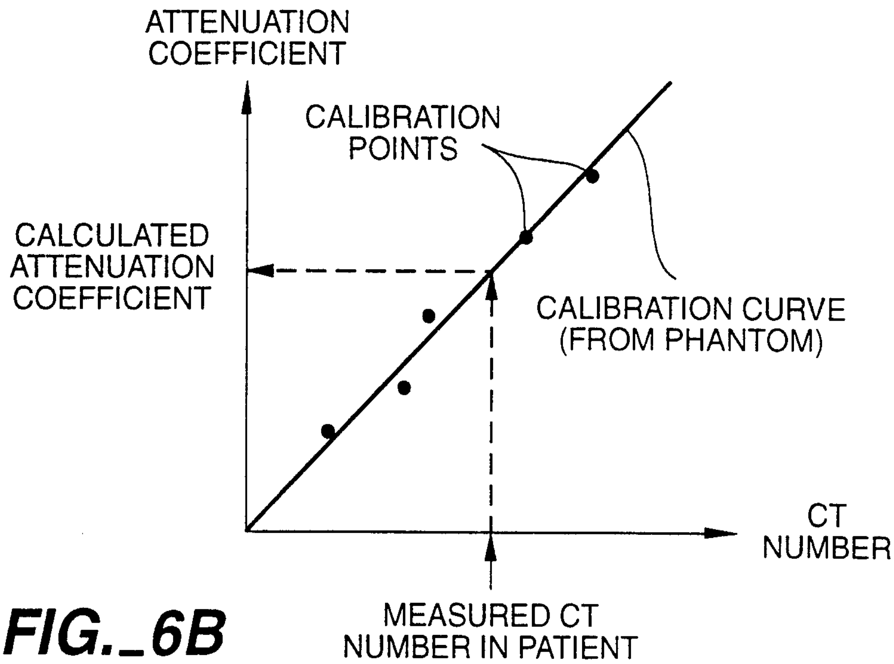
ATTENUATION
COEFFICIENT
CALIBRATION
POINTS
CALCULATED
ATTENUATION
COEFFICIENT
CALIBRATION CURVE
(FROM PHANTOM)
CT
NUMBER
MEASURED CT
NUMBER IN PATIENT

FIG._6B

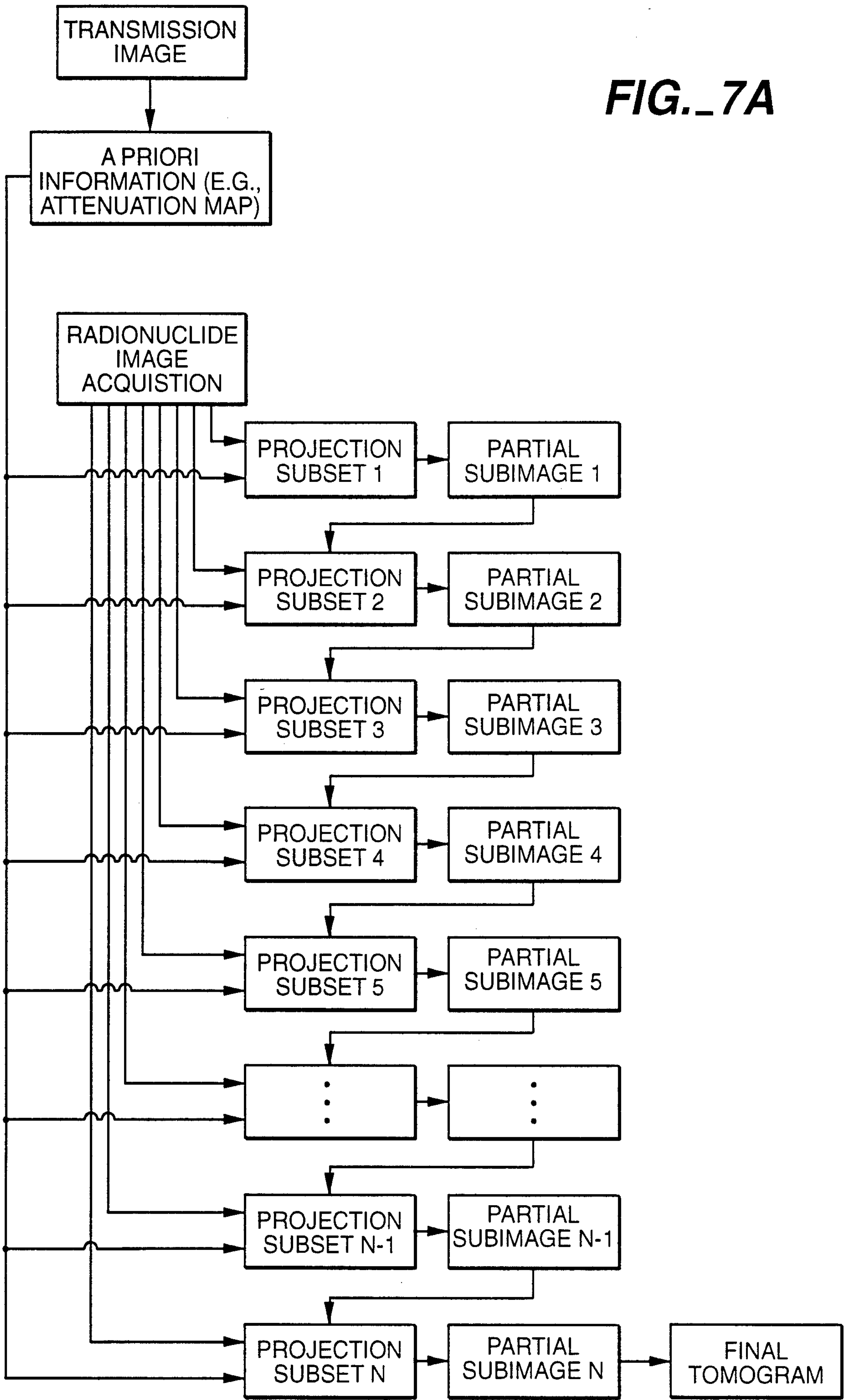
TRANSMISSION IMAGE
A PRIORI INFORMATION (E.G., ATTENUATION MAP)
RADIONUCLIDE IMAGE ACQUISTION
PROJECTION SUBSET 1
PARTIAL SUBIMAGE 1
PROJECTION SUBSET 2
PARTIAL SUBIMAGE 2
PROJECTION SUBSET 3
PARTIAL SUBIMAGE 3
PROJECTION SUBSET 4
PARTIAL SUBIMAGE 4
PROJECTION SUBSET 5
PARTIAL SUBIMAGE 5
PROJECTION SUBSET N-1
PARTIAL SUBIMAGE N-1
PROJECTION SUBSET N
PARTIAL SUBIMAGE N
FINAL TOMOGRAM

FIG._7A

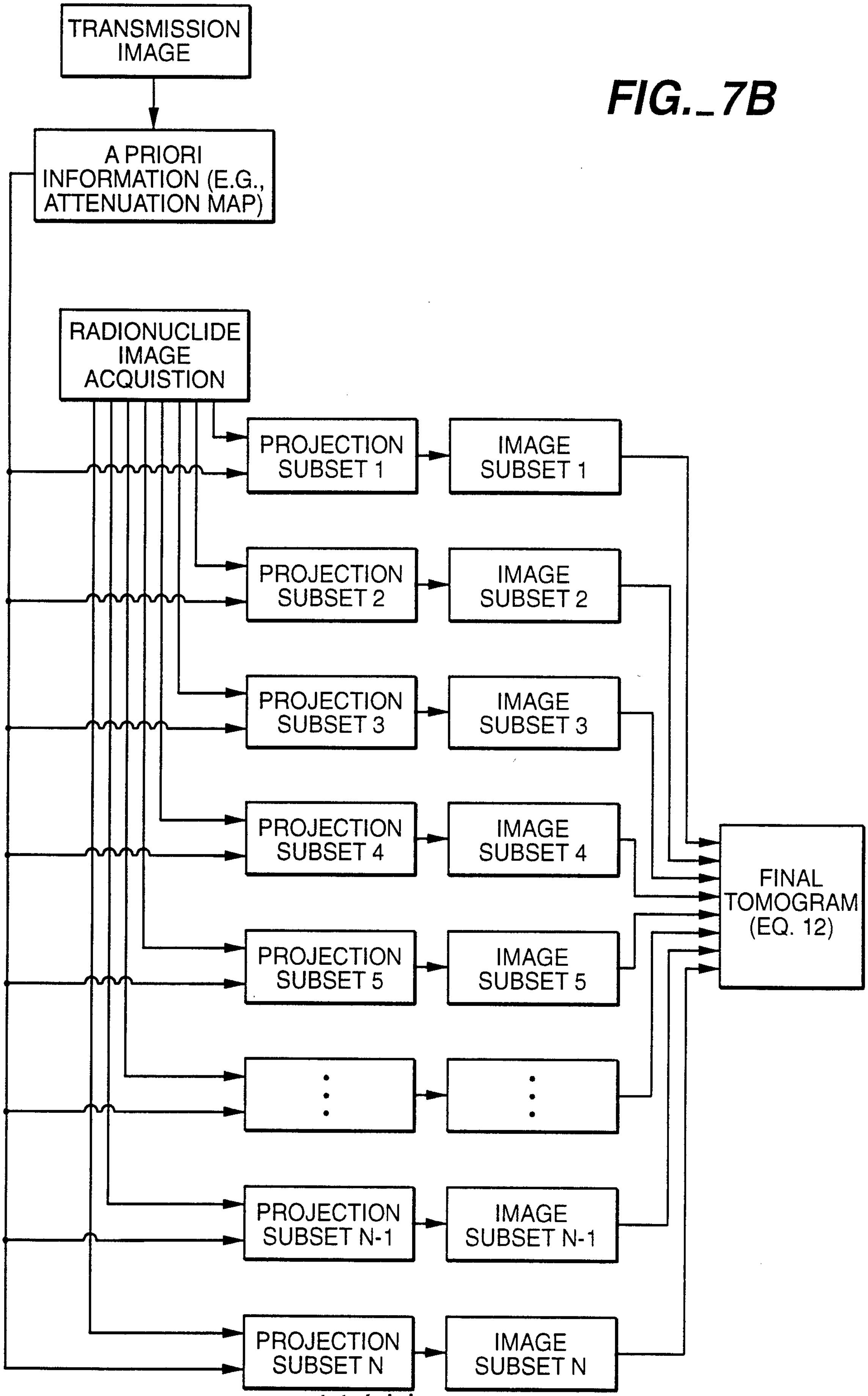
TRANSMISSION IMAGE
A PRIORI INFORMATION (E.G., ATTENUATION MAP)
RADIONUCLIDE IMAGE ACQUISTION
PROJECTION SUBSET 1
IMAGE SUBSET 1
PROJECTION SUBSET 2
IMAGE SUBSET 2
PROJECTION SUBSET 3
IMAGE SUBSET 3
PROJECTION SUBSET 4
IMAGE SUBSET 4
PROJECTION SUBSET 5
IMAGE SUBSET 5
PROJECTION SUBSET N-1
IMAGE SUBSET N-1
PROJECTION SUBSET N
IMAGE SUBSET N
FINAL TOMOGRAM (EQ. 12)

FIG._7B

INTERNATIONAL SEARCH REPORT

International application No.
PCT/US93/09429

A. CLASSIFICATION OF SUBJECT MATTER

IPC(5) :GOIT 1/166
US CL :250/363.04; 364/413.19, 413.21, 413.22, 413.24
According to International Patent Classification (IPC) or to both national classification and IPC

B. FIELDS SEARCHED

Minimum documentation searched (classification system followed by classification symbols)

U.S. : 250/363.04; 364/413.19, 413.21, 413.22, 413.24

Documentation searched other than minimum documentation to the extent that such documents are included in the fields searched

none

Electronic data base consulted during the international search (name of data base and, where practicable, search terms used)

none

C. DOCUMENTS CONSIDERED TO BE RELEVANT

Category*	Citation of document, with indication, where appropriate, of the relevant passages	Relevant to claim No.
X	US,A 4,633,398 (GULBERG ET AL.) 30 December 1986. See col. 12, lines 1-64	1-8, 12-21 28-30
X,P	US,A 5,210,421 (GULBERG ET AL.) 11 May 1993. See col. 3, lines 9-10; col. 6, lines 43-53, col. 7, lines 21-25; col. 8, lines 27-32	1-8, 12-21 28-30

☐ Further documents are listed in the continuation of Box C. ☐ See patent family annex.

* Special categories of cited documents:

"A" document defining the general state of the art which is not considered to be part of particular relevance

"E" earlier document published on or after the international filing date

"L" document which may throw doubts on priority claim(s) or which is cited to establish the publication date of another citation or other special reason (as specified)

"O" document referring to an oral disclosure, use, exhibition or other means

"P" document published prior to the international filing date but later than the priority date claimed

"T" later document published after the international filing date or priority date and not in conflict with the application but cited to understand the principle or theory underlying the invention

"X" document of particular relevance; the claimed invention cannot be considered novel or cannot be considered to involve an inventive step when the document is taken alone

"Y" document of particular relevance; the claimed invention cannot be considered to involve an inventive step when the document is combined with one or more other such documents, such combination being obvious to a person skilled in the art

"&" document member of the same patent family

Date of the actual completion of the international search	Date of mailing of the international search report
01 DECEMBER 1993	10 DEC 1993

Name and mailing address of the ISA/US	Authorized officer
Commissioner of Patents and Trademarks Box PCT Washington, D.C. 20231	CAROLYN E. FIELDS
Facsimile No. NOT APPLICABLE	Telephone No. (703) 308-4860

Form PCT/ISA/210 (second sheet)(July 1992)★

INTERNATIONAL SEARCH REPORT

International application No.
PCT/US93/09429

Box I Observations where certain claims were found unsearchable (Continuation of item 1 of first sheet)

This international report has not been established in respect of certain claims under Article 17(2)(a) for the following reasons:

1. ☐ Claims Nos.:
because they relate to subject matter not required to be searched by this Authority, namely:

2. ☐ Claims Nos.:
because they relate to parts of the international application that do not comply with the prescribed requirements to such an extent that no meaningful international search can be carried out, specifically:

3. ☐ Claims Nos.:
because they are dependent claims and are not drafted in accordance with the second and third sentences of Rule 6.4(a).

Box II Observations where unity of invention is lacking (Continuation of item 2 of first sheet)

This International Searching Authority found multiple inventions in this international application, as follows:
(Form PCT/ISA/206 Previously Mailed.)
Please See Extra Sheet.

1. ☐ As all required additional search fees were timely paid by the applicant, this international search report covers all searchable claims.

2. ☐ As all searchable claims could be searched without effort justifying an additional fee, this Authority did not invite payment of any additional fee.

3. ☐ As only some of the required additional search fees were timely paid by the applicant, this international search report covers only those claims for which fees were paid, specifically claims Nos.:

4. ☒ No required additional search fees were timely paid by the applicant. Consequently, this international search report is restricted to the invention first mentioned in the claims; it is covered by claims Nos.:
1-21, 28-30

Remark on Protest ☐ The additional search fees were accompanied by the applicant's protest.
☐ No protest accompanied the payment of additional search fees.

BOX II. OBSERVATIONS WHERE UNITY OF INVENTION WAS LACKING
This ISA found multiple inventions as follows:

I. Claims 1-21 and 28-30, drawn to an emission-transmission imaging system and a method of forming an emission image, classified in Class 250, subclass 363.04.
II. Claims 22-27, drawn to a method of computed tomography image reconstruction, classified in Class 378, subclass 4.

Inventions I and II are related as combination and subcombination. The combination as claimed does not require the particulars of the subcombination as claimed because the subcombination of claim 22 requires that the CT image be reconstructed by using subsets of electrical signals but parent claims 1 and 28 do not require use of subsets. Thus, the invention are not so linked as to form a single general inventive concept.